# ACP5, TNF, and MMP8 were identified as potential biomarkers of steroid-induced osteonecrosis of the femoral head

**Jian Zhang**
Department of Orthopedics, The Second Affiliated Hospital of Harbin Medical University
**Zehan Liu**
Department of Orthopedics, The Second Affiliated Hospital of Harbin Medical University
**Shuai Ren**
Department of Orthopedics, The Second Affiliated Hospital of Harbin Medical University
**Zilong Shen**
Department of Orthopedics, The Second Affiliated Hospital of Harbin Medical University
**Kecheng Han**
Department of Orthopedics, The fifth Hospital of Harbin
**Weiguang Xin**
Department of Orthopedics,The Second Hospital of Heilongjiang Province
**Guanyi He**
Department of Orthopedics, The Second Affiliated Hospital of Harbin Medical University
**Chi Huang**
Department of Orthopedics, The Second Affiliated Hospital of Harbin Medical University
**Jianyu Liu** ( liujianyu4@163.com )
Department of Orthopedics, The Second Affiliated Hospital of Harbin Medical University

**Research Article**

**Keywords:** Steroid-induced osteonecrosis of the femoral head, Candidate genes, ceRNA network, Bioinformatics

**Posted Date:** May 27th, 2021

**DOI:** https://doi.org/10.21203/rs.3.rs-94892/v2

# ACP5, TNF, and MMP8 were identified as potential biomarkers of steroid-induced osteonecrosis of the femoral head

Jian Zhang[1], Zehan Liu[1], Shuai Ren[1], Zilong Shen[1], Kecheng Han[2], Weiguang Xin[3], Guanyi He[1], Chi Huang[1], Jianyu Liu[1,*]

[1] Department of Orthopedics, The Second Affiliated Hospital of Harbin Medical University, Harbin, 150001, Heilongjiang, China

[2] Department of Orthopedics, The fifth Hospital of Harbin, Harbin, 150040, Heilongjiang, China

[3] Department of Orthopedics,The Second Hospital of Heilongjiang Province, Harbin, 150000, Heilongjiang, China

[*] Author for correspondence

## Abstract

Steroid-induced osteonecrosis of the femoral head (SONFH) is a progressive bone disorder that is characterized by femoral head collapse and hip joint dysfunction. To elucidate the biomarkers of SONFH, the GSE123568 dataset was downloaded from the Gene Expression Omnibus (GEO) database. A total of 436 differentially expressed SONFH genes were screened in comparison with non-SONFH genes. Six biological processes and four KEGG pathways were enriched in SONFH by GSEA,

and 68 candidate genes that were involved in these pathways were selected for subsequent analysis. Moreover, through an ingenuity pathway analysis, we obtained 10 canonical pathways and 20 molecule function modules related to SONFH, and acquired 121 candidate genes. Furthermore, we identified ACP5, TNF, and MMP8 as the genes most related to SONFH according to the VarElect and MalaCards database. Based on these hub genes, the targeted miRNAs and the lncRNAs were predicted. Finally, the ceRNA network was constructed by using ACP5, TNF, MMP8, seven miRNAs, and 956 candidate lncRNAs. In conclusion, the ACP5, TNF, and MMP8 might be potential biomarkers of SONFH.

**Keywords:** Steroid-induced osteonecrosis of the femoral head, Candidate genes, ceRNA network, Bioinformatics

## 1. Introduction

Osteonecrosis of the femoral head (ONFH), which is also called avascular necrosis (AVN) of the femoral head, is an increasing health problem in the world. ONFH refers to progressive necrosis of osteocytes and bone marrow elements, and the clinical symptoms include grievous pain and limping gait[1]. Steroid administration is the main cause of ONFH, and it occurs in 51%–60% of all cases of ONFH [2, 3]. The etiology and pathological process of SONFH are complex. Oxidative stress [1], osteoclasts activation [4], and bone-metabolism disorder [5] have been correlated with SONFH. However, the exact molecular mechanisms of SONFH remain unclear.

Although, magnetic resonance imaging (MRI) is a valid method for diagnosing SONFH [3], some patients were misdiagnosed due to the complexity of their clinical manifestations. Therefore, reliable diagnostic biomarkers of SONFH are urgently needed.

A recent study demonstrated that the osteoclastic-related genes OPG and RANML were abnormally expressed in SONFH, and therefore, they are potential diagnostic markers[6]. However, other processes, including coagulopathy[7], dysregulated apoptosis[8], and disordered lipid metabolism[9] were also crucial for SONFH. In addition, inflammatory pathways such as the PDK1/AKT/mTOR signaling pathway and the PERK and Parkin pathways [10, 11] are utilized for the function of dysregulated genes in these function pathways might act as potential biomarkers of SONFH.

Non-coding RNAs have been identified as regulators of gene expression and physiological process. In SONFH, studies have shown that miRNAs are aberrantly expressed in necrotic tissue[12], serum[13], bone marrow mesenchymal stem cells[14], and osteoblasts[15]. Abnormal miRNA expression causes dysregulation of genes. ncRNAs and lncRNAs, which act as competing endogenous RNAs (ceRNAs) of miRNAs[16], have rarely been investigated in SONFH. Xiang et al. found that lncRNA RP11-154D6 impacted the progress of SONFH by promoting osteogenic differentiation and inhibiting adipogenic differentiation in BMSCs [17]. lncRNA RP1-193H18.2, MALAT1, and HOTAIR have been associated with abnormal osteogenic and adipogenic differentiation of BMSCs in SONFH [18]. However, the

mechanisms of lncRNA in SONFH have yet to be discovered. Revealing the associations among mRNA, miRNA, and lncRNA in the ceRNA network of SONFH can elucidate activities at the molecular level that would lead to uncovering new targets for therapy and diagnosis.

In our study, we analyzed the function pathways in SONFH based on differentially expressed genes and screened hub genes to predict miRNA and lncRNA to construct a ceRNA network in SONFH. Our study revealed candidate biomarker genes and potential regulated pathways of SONFH.

## 2. Materials and methods

### 2.1 Data download and processing

We downloaded data on the gene expression profiles of SONFH from the Gene Expression Omnibus (GEO) database (*http://www.ncbi.nlm.nih.gov/geo/*). Dataset GSE123568 was performed on the Affymetrix human gene expression array, including a total of 40 peripheral serum specimens (30 SONFH patients and 10 non-SONFH individuals). The background correction of raw data were processed by robust multiarray average (RMA), and the signals were log2 transformed and normalized through quantile normalization. After that, qualified transcriptome data were used for future analyses.

### 2.2 Gene set enrichment analysis

To explore the functional phenotypes between SONHF and non-SONFH, we first used the “limma”R package to screen the differentially expressed genes (DEGs) between these two groups in the GSE123568 dataset. The screening standard was $|\log_2 FC|>=1$ and $p < 0.05$. Then, we performed gene set enrichment analysis (GSEA) by using “c5.all.v7.1.symbols.gm” and “c2.cp.kegg.v7.1.symbols.gm” as the reference gene set. In addition to adopting the default parameter, larger sets > 500 and smaller sets < 15 were excluded, as additional parameter settings for filtering enriched gene sets. A false discovery rate (FDR) < 0.25 and $p < 0.05$ were considered significant. Genes participating in significant pathways were selected as candidate genes.

**2.3 Ingenuity pathway analysis**

The ingenuity pathway analysis (IPA) system was used for core analysis based on the DEGs to determine the function pathways involved in SONFH. Analyses including screening canonical pathways were used to explore the relationship between the gene function and diseases, $|z\text{-score}| > 2$ and $p < 0.05$ were set as the standard. Genes that were involved in significant pathways were obtained as candidate genes.

**2.4 Identification of SONFH-related genes**

To identify SONFH-related genes, we first integrated candidate genes. Then, the VarElect online tool (http://ve.g.,enecards.org) was implemented to select the genes most strongly associated by score.oreover, MalaCards database

(http://www.malacards.org/) was utilized to acquire genes correlated to osteonecrosis. Finally, SONFH-related genes were identified by the two intersecting methods, and mutual genes were obtained.

### 2.5 Construction of a ceRNAs network

miRWalk (http://mirwalk.umm.uni-heidelberg.de/) was used to predict the target mRNA of miRNA, and the interaction between miRNA and lncRNA was predicted by DIANA-LncBASE Predicted v2 (http://carolina.imis.athena-innovation.gr/diana_tools/web/index.php?r=lncbasev2 / index-predicted). Then, Cytoscape 3.6.1 software was employed for ceRNAs networks visualization.

## 3.Results

### 3.1 DEG identification and pathway enrichment by GSEA

After data preprocessing and screening under the threshold of $|\log_2 FC|>=1$ and $p <=0.05$, a total of 436 DEGs (216 down-regulated and 220 up-regulated) were obtained for subsequent analysis. Then, GSEA was conducted to enrich pathways in SONFH under the threshold of FDR < 0.25 and $p < 0.05$. The results of the GSEA showed that programmed necrotic cell death, necrotic cell death, and intracellular lipid transport were activated in SONFH (Figures 1A-C), but the lymph vessel morphogenesis, lymph vessel development, and hydrogen peroxide catabolic process were suppressed (Figures 1D–F). In addition, leishmania infection, the T cell

receptor signaling pathway, and glycosaminoglycan biosynthesis chondroitin sulfate were significantly up-regulated in SONFH, whereas porphyrin and chlorophyll metabolism were down-regulated (Figures 2A–D). Sixty-eight genes involved in these pathways were selected as candidate genes of SONFH (Table 1).

### 3.2 Candidate genes identified by IPA

To obtain candidate SONFH-related-genes, DEGs were also employed for IPA core analysis with a filter of $p < 0.05$ and $|z\text{-score}| > 2$. We found that nitric oxide (NO) and reactive oxygen species (ROS) production in mφ, Fcγ receptor-mediated phagocytosis in mφ and monocytes, type I interferons (IFN), Tec kinase, TREM1, Gai, iNOS, and neuroinflammation signaling routing, and dendritic cell development were enhanced as $|z\text{-score}| > 2$. The signaling pathway of sirtuin was inhibited as a $|z\text{-score}| < 2$ in SONFH (Figure 3A, table 2). Among them, production of NO and ROS in mφ obtained a $z$-score = 3.464 as the highest positive score. The 12 genes screened from this pathway are shown in table 2.

Moreover, based on the disease and function analysis, we found that the DEGs were collected in different pathways (Figure 3B). Of 48 functional modules, 20 were filtered by $p < 0.05$ and $|z\text{-score}| > 2$, and identified as strongly correlated to SONFH (Figure 3C).

### 3.3 Identification of SONFH-related genes

To identify the hub genes of SONFH, we first integrated the candidate genes screened by GESA and PIA and uploaded them into the VarElect online tool. The

result showed that TNF acquired the highest correlation score; TNFSF10, FAS, TNFSF13B, and FASLG obtained a higher correlation score than that of the other candidate genes (Table 3). Then, 32 osteonecrosis-related candidate genes were selected from the MalaCards database (Table 4). Finally, ACP5, TNF, and MMP8 as SONFH-related genes were selected using the Venn diagram (Figure 4).

### 3.4 Construction of the ceRNA network of SONFH-related genes

To explore the regulatory mechanism of ACP5, TNF, and MMP8 in SONFH, ceRNAs networks including genes, miRNA, and lncRNA were established. Then, 372, 795, and 265 miRNAs were targeted to ACP5, TNF, and MMP8, respectively. By overlapping these miRNAs, we found that hsa-miR-1587, hsa-miR-4653-5p, hsa-miR-7845-5p, hsa-miR-5010-3p, and hsa-miR-6772-3p were linked with all three genes (Figure 5A). Moreover, the miRNAs that were supported by experimental evidence were also selected in the ceRNAs network, including hsa-miR-452-5p, hsa-miR-130a-3p, hsa-miR-19a-3p, hsa-miR-187-3p, hsa-miR-143-3p (targeted to TNF), and has-miR-26b-5p (targeted to MMP8) (Table 5). In addition, lncRNAs targeted to the 11 miRNAs were predicted to form regulatory modules. As a result,, 956 candidate lncRNAs were connected with seven candidate miRNAs (Figure 5B, table 6).

### 3.5. Discussion

SONFH is a progressive bone disease caused by steroid treatment that results in mechanism stress damage, vascular injury, intraosseous pressure enhancing,

adipocyte activated, coagulation, and apoptosis dysfunction[3]. The credible biomarker of SONFH is still unknown. In the present study, we enriched the biological function and pathway related to SONFH by clusterProfiler, ClueGO, IPA, and GSEA analyses. In the future, SONFH-related genes were screened by the VarElect and the MalaCards databases. Finally, ACP5, TNF, and MMP8 were identified as the most SONFH-related genes, and a ceRNA network was constructed for searching for the regulation mechanism in SONFH

Previous studies indicated that ACP5 is expressed in many types of differentiated cells, such as granulocytes, dendritic cells, macrophages, and osteoclasts[19-21]. ACP5 is a histochemical marker for osteoclasts[22]. Furthermore, ACP5 is a multifunctional protein that is necessary for novel bone development, osteoclast differentiation, bone resorption, and osteoclast activity[23]. Since ACP5 has a physiological expression, its pathological expression in different human conditions appears to be reasonable[23]. Recently, a study revealed that ACP5 declined in ONFH tissues and was regulated by Wnt-11 and miR-410[24]. This was in accord with our results that demonstrated that ACP5 was down-regulated in SONFH. Therefore, ACP5 is a potential biomarker for SONFH. Interestingly, TNF, which is one of the biomarker genes that is involved in the RANKL-NFATc1/c-FOS signaling pathway, induced ACP5 transcription to accelerate osteoclastogenesis[25]. In defining the function mechanism, scientists have reached an agreement that TNF-α inhibits collagen synthesis, AKP activity, and osteocalcin synthesis[26]. Moreover, TNF exhibits elevated expression and is positively correlated with ADAMTS-7 to

exaggerate cartilage degeneration in ONFH[27]. After further exploration, we found that TNF was enriched in SONFH and showed a significant interaction of SONFH.

Matrix metalloproteinase-8 (MMP-8) is included in a family of zinc-dependent proteolytic enzymes and is intensely expressed along to promote and improve osteoblast development into osteocytes[28]. A previous study[29] suggested that genetic variations of the MMP/TIMP system could induce aberrant activation of osteoclasts and cause ONFH. Jieli Du's report considered that genetic variants of MMP8 are conductive to steroid-induced ONFH susceptibility in northern China[30]. We did not detect genetic polymorphisms of MMP8 in our study, but the decreased expression of MMP8 might be associated with genetic variants.

To further investigate the regulation mechanism of gens in SONFH, we constructed a ceRNA network that included genes, miRNA, and lncRNA. The miRNAs were predicted by hub genes acting as target genes, and the results showed that 372 miRNAs were targeted to ACP5, 795 miRNAs were related to TNF, and four miRNAs were linked with MMP8. Among them, hsa-miR-6772-3p, hsa-miR-7845-5p, hsa-miR-4653-5p, hsa-miR-5010-3p, and hsa-miR-1587 were linked to all three (MMP8, ACP5, and TNF). Then, these miRNAs combined with miRNAs were supported with experimental evidence to predicate the lncRNAs, and we screened hsa-miR-5010-3p, hsa-miR-26b-5p, hsa-miR-19a-3p, hsa-miR-452-5p, hsa-miR-187-3p, hsa-miR-130a-3p, and hsa-miR-143-3p to construct ceRNAs networks with ACP5, TNF, MMP8, and lncRNAs. None of the previous research had reported this ceRNAs network in SONFH, and the mechanism requires future

analyses to verify our findings.

## 4.Conclusion

In summary, by using bioinformatics analyses, we unveiled three genes that are significantly associated with SONFH and constructed a ceRNA network to prove a potential pathogenesis and treatment for this disease.

## References

1. Chen, K., et al., Steroid-induced osteonecrosis of the femoral head reveals enhanced reactive oxygen species and hyperactive osteoclasts. International journal of biological sciences, 2020. 16(11): p. 1888-1900.
2. Fukushima, W., et al., Nationwide epidemiologic survey of idiopathic osteonecrosis of the femoral head. Clinical orthopaedics and related research, 2010. 468(10): p. 2715-2724.
3. Chang, C., A. Greenspan, and M.E. Gershwin, The pathogenesis, diagnosis and clinical manifestations of steroid-induced osteonecrosis. Journal of autoimmunity, 2020. 110: p. 102460.
4. Zhou, Z., et al., IL-15 deficiency alleviates steroid-induced osteonecrosis of the femoral head by impact osteoclasts via RANKL-RANK-OPG system. Immunity & ageing: I & A, 2020. 17: p. 19.
5. Tian, L., et al., Imbalanced bone turnover markers and low bone mineral density in

patients with osteonecrosis of the femoral head. International orthopaedics, 2018. 42(7): p. 1545-1549.

6. Min-Cong He, et al., Osteoclastic activity was associated with the development of steroid-induced osteonecrosis of femoral head.Artif Cells Nanomed Biotechnol.2020 Dec;48(1):1036-1046.

7. Yong Feng, et al., Decreased in the number and function of circulation endothelial progenitor cells in patients with avascular necrosis of the femoral head.Bone. 2010 Jan;46(1):32-40.

8. Zhen-Qun Zhao, et al.,Mechanism of Methylprednisolone-Induced Primary Cilia Formation Disorder and Autophagy in Osteoblasts.Orthop Surg. 2020 Apr;12(2):645-652.

9. Tetsurou Hirata, et al., ApoB C7623T polymorphism predicts risk for steroid-induced osteonecrosis of the femoral head after renal transplantation.J Orthop Sci. 2007 May;12(3):199-206.

10. Wen-Ning Xu., et al., HIF-1α Regulates Glucocorticoid-Induced Osteoporosis Through PDK1/AKT/mTOR Signaling Pathway. Front Endocrinol (Lausanne). 2020 Jan 28;10:922.

11. Yanchun Gao. et al., Inhibition of PERK Signaling Prevents Against Glucocorticoid-induced Endotheliocyte Apoptosis and Osteonecrosis of the Femoral Head. Int J Biol Sci. 2020 Jan 1;16(4):543-552.

12. Chao P.-C., Cui M.-Y., Li X.-A., Jiang Y., Lin B.-C., Li Z.-B. Correlation between miR-1207-5p expression with steroid-induced necrosis of femoral head and

VEGF expression. European Review for Medical and Pharmacological Sciences. 2019;23(7):2710–2718.

13.Li Z., Jiang C., Li X., et al. Circulating microRNA signature of steroid-induced osteonecrosis of the femoral head. Cell Proliferation. 2018;51(1).

14.Zhao S. R., Wen J. J., Mu H. B. Role of Hsa-miR-122-3p in steroid-induced necrosis of femoral head. European Review for Medical and Pharmacological Sciences. 2019;23(3 Suppl):54–59.

15.Li P., Sun N., Zeng J., et al. Differential expression of miR-672-5p and miR-146a-5p in osteoblasts in rats after steroid intervention. Gene. 2016;591(1):69–73.

16.Wu, X., W. Sun, and M. Tan, Noncoding RNAs in Steroid-Induced Osteonecrosis of the Femoral Head. BioMed research international, 2019. 2019: p. 8140595.

17.Xiang, S., Z. Li, and X. Weng, The role of lncRNA RP11-154D6 in steroid-induced osteonecrosis of the femoral head through BMSC regulation. Journal of cellular biochemistry, 2019. 120(10): p. 18435-18445.

18.Wang, Q., et al., LncRNA expression profiling of BMSCs in osteonecrosis of the femoral head associated with increased adipogenic and decreased osteogenic differentiation. Scientific reports, 2018. 8(1): p. 9127.

19.A R Hayman., et al., Osteoclastic tartrate-resistant acid phosphatase (Acp 5): its localization to dendritic cells and diverse murine tissues.J Histochem Cytochem. 2000 Feb;48(2):219-28.

20.A R Hayman., et al., Tartrate-resistant acid phosphatase (Acp 5): identification in diverse human tissues and dendritic cells. J Histochem Cytochem. 2001 Jun;49(6):675-84.

21.C Minkin., Bone acid phosphatase: tartrate-resistant acid phosphatase as a marker of osteoclast function. Calcif Tissue Int. 1982 May;34(3):285-90.

22.M S Burstone., Histochemical demonstration of acid phosphatase activity in osteoclasts. J Histochem Cytochem. 1959 Jan;7(1):39-41.

23.Xin Ren., et al., ACP5: Its Structure, Distribution, Regulation and Novel Functions.Anticancer Agents Med Chem. 2018;18(8):1082-1090.

24.Yukun Yin., et al., Upregulating MicroRNA-410 or Downregulating Wnt-11 Increases Osteoblasts and Reduces Osteoclasts to Alleviate Osteonecrosis of the Femoral Head. Nanoscale Res Lett. 2019 Dec 18;14(1):383.

25.Hiroshi Takayanagi., et al.,Induction and activation of the transcription factor NFATc1 (NFAT2) integrate RANKL signaling in terminal differentiation of osteoclasts. Dev Cell. 2002 Dec;3(6):889-901.

26.Yaosheng Liu., et al., Combined effect of tnf-α polymorphisms and hypoxia on steroid-induced osteonecrosis of femoral head. Int J Clin Exp Pathol. 2015 Mar 1;8(3):3215-9.

27.Jing-kun Li., et al., ADAMTS-7 exhibits elevated expression in cartilage of osteonecrosis of femoral head and has a positive correlation with TNF- α and NF- κ B P65.Mediators Inflamm. 2015;2015:196702.

28.M Tsubota., et al., Expression of MMP-8 and MMP-13 mRNAs in rat

periodontium during tooth eruption. J Dent Res. 2002 Oct;81(10):673-8.

29. Susanne Grässel., et al., Expression profile of matrix metalloproteinase-2 and -9 and their endogenous tissue inhibitors in osteonecrotic femoral heads. Int J Mol Med. 2010 Jul;26(1):127-33.

30. Jieli Du., et al., Association between genetic polymorphisms of MMP8 and the risk of steroid-induced osteonecrosis of the femoral head in the population of northern China. Medicine (Baltimore). 2016 Sep;95(37):e4794.

**Table 1.** Key enrichment pathways and pathway-involved genes by GSEA

| Enrichment pathway | Gene symbols of core enrichment |
|---|---|
| programmed necrotic cell death | PELI1, TICAM2, CD14, MAP3K5, TLR4, LY96, CFLAR, BIRC3, FAS, MLKL, CASP8, PPIF, PYGL, RIPK1, CYLD, ITPK1, TICAM1, FASLG, RBCK1, TLR3, TNF |
| intracellular lipid transport | ABCG1, PRKAG2, CPT1B, ABCA1, MID1IP1, SGPP1, CES1, ANXA2P2, SERAC1, NPC1, OSBPL2, ANXA2, ABCD3, CPT2, SLC25A20, LDLRAP1, NPC2, NUS1 |
| necrotic cell death | PELI1, TICAM2, CD14, MAP3K5, TLR4, LY96, CFLAR, BIRC3, FAS, MLKL, CASP8, PPIF, PYGL, TMEM123, RIPK1, HEBP2, CYLD, ITPK1, TICAM1, FASLG, RBCK1, TLR3, TNF, TSPO |
| lymph vessel morphogenesis | FLT4, ACVRL1, PDPN, PPP3CB, EPHA2, FOXC1, PROX1, CCBE1, PROX2, VEGFC, SOX18 |
| hydrogen peroxide catabolic process | EPX, CAT, APOA4, MT3, GPX5, HBM, HBQ1, HBE1, HBZ, MPO, HP, PXDN, SNCA, PRDX2, HBD |
| lymph vessel development | TBX1, FLT4, EFNB2, ACVRL1, PDPN, PPP3CB, EPHA2, FOXC1, PROX1, CCBE1, PROX2, VEGFC, SOX18 |
| leishmania infection | PTGS2, TLR2, NCF1, HLA-DMB, NCF4, NCF2, TLR4, HLA-DRB3, IFNGR1, JAK2, IFNGR2, FCGR2A, FCGR2C, HLA-DMA, ITGB2, ITGA4, MAPK3, PTPN6, FCGR3A, HLA-DRB5, IL1B, JAK1, TRAF6, PRKCB, FCGR3B, ITGAM, CYBA, HLA-DRA, STAT1, NFKBIA, HLA-DRB1, HLA-DPA1, TGFB1, NFKB1, MYD88, FOS, HLA-DOB, HLA-DQA2, IRAK1, HLA-DRB4, MAPK14, TNF, HLA-DQA1 |
| glycosaminoglycan biosynthesis chondroitin sulfate | CHST7, CHST15, CSGALNACT1, XYLT1, CHSY1, DSE, CHST11, CHST14, B3GALT6, CSGALNACT2 |
| T cell receptor signaling pathway | MAP3K8, PAK1, ICOS, RAF1, LCP2, PIK3R5, CBL, MALT1, MAPK3, PTPN6, BCL10, PAK2, SOS2, CHUK, PIK3CB, NFKBIE, LCK, PTPRC, VAV1, NCK1, LAT, CD28, ITK, NFKBIA, MAP2K1, PIK3CG, GSK3B, PIK3CD, PDPK1, CD3D, NFKB1, NFATC3, CD4, GRB2,CD3G, FOS, FYN, |
| | IKBKB, PPP3CA, CD8B, RASGRP1, PLCG1, MAP3K14, RHOA, AKT1, CD8A, CD247, CD3E, MAPK14, TNF, SOS1, PPP3CC, KRAS, PRKCQ, AKT3, CARD11 |
| porphyrin and chlorophyll | CP, UGT2B10, UROS, CPOX, UGT1A1, UGT1A10, UGT1A3, UGT1A6, UGT1A4, UGT1A5, UGT1A7, UGT1A8, UGT1A9, UGT2B4, BLVRB, PPOX, FTMT, ALAD, ALAS2, UROD, UGT2B28, HMBS, UGT2B7, |

| | |
|---|---|
| metabolism | FECH |

**Table 2**. Core analysis of the DEGs matrix using IPA in SONFH.

| Ingenuity canonical pathway | -log (p value) | Ratio | z-score | Molecules |
|---|---|---|---|---|
| Interferon Signaling | 4.12 | 0.167 | 2.449 | IFIT1, IFIT3, IFNGR1, IFNGR2, MX1, TYK2 |
| Production of Nitric Oxide and Reactive Oxygen Species in Macrophages | 3.41 | 0.0649 | 3.464 | ARG2, IFNGR1, IFNGR2, IRF8, LYZ, NCF1, NCF2, NCF4, RHOQ, SERPINA1, TLR2, TYK2 |
| Fcγ Receptor-mediated Phagocytosis in Macrophages and Monocytes | 2.56 | 0.0753 | 2.646 | FCGR2A, FCGR3A/FCGR3B, HCK, LCP2, LYN, NCF1, PAK1 |
| TREM1 Signaling | 2.54 | 0.0857 | 2.449 | TLR1, TLR2, TLR7, TLR8, TREM1, TYROBP |
| iNOS Signaling | 1.93 | 0.0909 | 2 | CD14, IFNGR1, IFNGR2, TYK2 |
| Gαi Signaling | 1.87 | 0.056 | 2.646 | CXCR2, FPR2, GNG11, HCAR2, P2RY13, RAP1GAP, S1PR3 |
| Neuroinflammation Signaling Pathway | 1.81 | 0.0412 | 2.333 | IFNGR1, IFNGR2, NCF1, NCF2, PTGS2, SNCA, TLR1, TLR2, TLR7, TLR8, TYK2, TYROBP |
| Tec Kinase Signaling | 1.79 | 0.05 | 2.449 | FCER1A, GNG11, HCK, LYN, PAK1, RHOQ, TNFSF10, TYK2 |
| Dendritic Cell Maturation | 1.61 | 0.0462 | 2.449 | FCGR2A, FCGR2C, FCGR3A/FCGR3B, HLA-DRB3, IGHG3, IRF8, TLR2, TYROBP |
| Sirtuin Signaling Pathway | 1.53 | 0.0389 | -2.333 | ARG2, BPGM, DUSP6, FOXO3, GABARAPL2, GADD45A, H1-2, MT-ND1, POLR1D, SLC2A1, STK11 |

**Table 3.** Candidate genes correlated to SONFH.

| Gene symbol | Description | Matched phenotypes | Score | Log10 (p) | Average disease causing likelihood |
|---|---|---|---|---|---|
| TNF | Tumor necrosis factor | Femoral head necrosis, necrosis | 116.56 | 4.42 | 70.40 |
| TNFSF10 | TNF superfamily member 10 | necrosis | 31.34 | 3.65 | 52.30 |
| FAS | Fas cell surface death receptor | necrosis | 26.35 | 3.42 | 44.30 |
| TNFSF13B | TNF superfamily member 13b | necrosis | 22.09 | 3.22 | 75.30 |
| FASLG | Fas ligand | necrosis | 21.95 | 3.19 | 63.40 |
| TLR4 | Toll like receptor 4 | necrosis | 19.41 | 3.08 | 25.40 |
| CASP8 | Caspase 8 | necrosis | 18.66 | 3.06 | 68.60 |
| RIPK1 | Receptor interacting serine/threonine kinase 1 | necrosis | 16.38 | 2.89 | 72.70 |
| PTGS2 | Prostaglandin endoperoxide synthase 2 | necrosis | 13.25 | 2.60 | 66.50 |

**Table 4.** Genes related to osteonecrosis in the MalaCards database.

| Gene symbol | Description | Score |
|---|---|---|
| BGLAP | Bone gamma-carboxyglutamate protein | 14.85 |
| TNFSF11 | TNF superfamily member 11 | 14.75 |
| BMP2 | Bone morphogenetic protein 2 | 14.67 |
| TNFRSF11B | TNF receptor superfamily member 11b | 14.60 |
| VEGFA | Vascular endothelial growth factor A | 14.34 |
| ACP5 | Acid phosphatase 5, tartrate resistant | 13.82 |
| COL2A1 | Collagen type Ⅱ alpha 1 chain | 13.80 |
| PTH | Parathyroid hormone | 13.80 |
| FDPS | Farnesyl diphosphate synthase | 13.79 |
| RUNX2 | Runx family transcription factor 2 | 13.73 |
| SERPINE1 | Serpin Family E Member 1 | 13.42 |
| MTHFR | Methylenetetrahydrofolate Reductase | 13.15 |
| CYP2C8 | Cytochrome P450 Family 2 Subfamily C Member 8 | 13.09 |
| F2 | Coagulation Factor II, Thrombin | 13.08 |
| TNF | Tumor Necrosis Factor | 13.06 |
| DKK1 | Dickkopf WNT Signaling Pathway Inhibitor 1 | 12.93 |
| ABCB1 | ATP Binding Cassette Subfamily B Member 1 | 12.85 |
| BMP7 | Bone Morphogenetic Protein 7 | 12.74 |
| NOS3 | Nitric Oxide Synthase 3 | 12.65 |
| NFATC1 | Nuclear Factor of Activated T Cells 1 | 12.56 |
| LRP5 | LDL Receptor Related Protein 5 | 12.49 |
| IGF1 | Insulin Like Growth Factor 1 | 12.45 |
| SERPINC1 | Serpin Family C Member 1 | 12.39 |
| CYP3A4 | Cytochrome P450 Family 3 Subfamily A Member 4 | 12.35 |

| | | |
|---|---|---|
| FAM201A | Family with Sequence Similarity 201 Member A | 12.34 |
| FGF2 | Fibroblast Growth Factor 2 | 12.33 |
| PLG | Plasminogen | 12.30 |
| ENG | Endoglin | 12.28 |
| MMP8 | Matrix Metallopeptidase 8 | 12.25 |
| BMP6 | Bone Morphogenetic Protein 6 | 12.14 |
| ESR1 | Estrogen Receptor 1 | 12.14 |
| IL10 | Interleukin 10 | 11.94 |

**Table 5.** Targets of hub genes with experimental evidence were predicated by miRWalk2.0.

| Gene symbol | miRNAs |
|---|---|
| ACP5 | / |
| MMP8 | hsa-miR-26b-5p |
| TNF | hsa-miR-452-5p |
| | hsa-miR-130a-3p |
| | hsa-miR-19a-3p |
| | hsa-miR-187-3p |
| | hsa-miR-143-3p |

**Table 6.** Targets of miRNAs were predicated by miRWalk2.0.

| Hub genes | Candidate miRNA | Predicated numbers of lncRNAs |
|---|---|---|
| ACP5/MMP8/TNF | hsa-miR-7845-5p | None |
| ACP5/MMP8/TNF | hsa-miR-6772-3p | None |
| ACP5/MMP8/TNF | hsa-miR-5010-3p | 124 |
| ACP5/MMP8/TNF | hsa-miR-4653-5p | None |
| ACP5/MMP8/TNF | hsa-miR-1587 | None |
| MMP8 | hsa-miR-26b-5p | 160 |
| TNF | hsa-miR-19a-3p | 220 |
| TNF | hsa-miR-452-5p | 66 |
| TNF | hsa-miR-187-3p | 19 |
| TNF | hsa-miR-130a-3p | 117 |
| TNF | hsa-miR-143-3p | 250 |

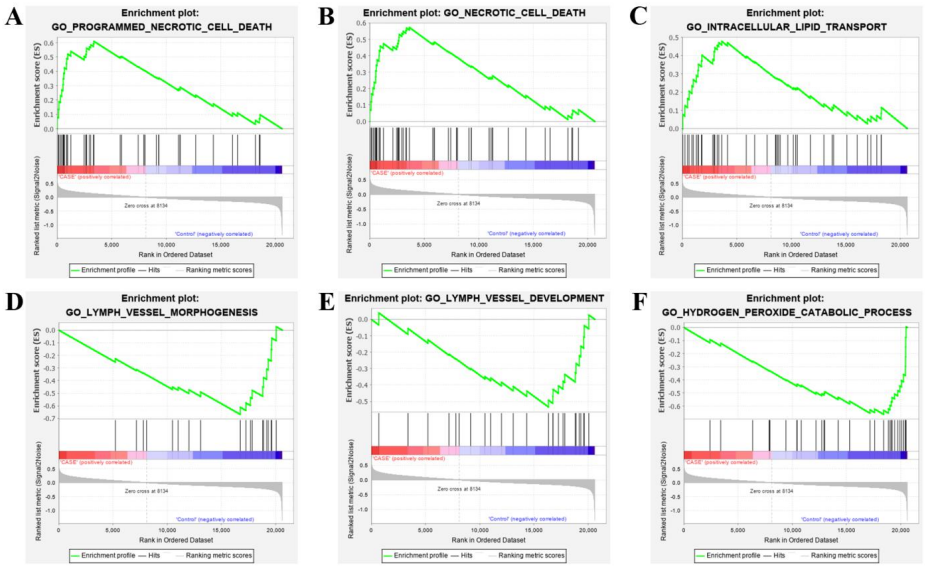


**Figure 1. Pathway enrichment by GSEA.** (A)-(F) The enriched entries were analyzed based on c5.all.v7.1.symbols.gm.

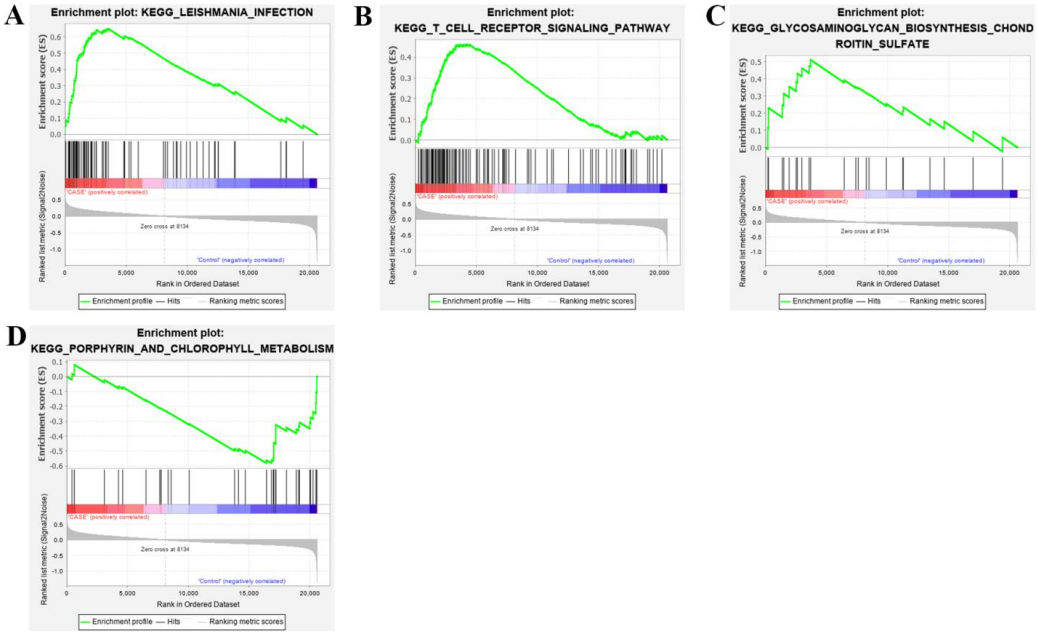


**Figure 2.** (A)-(D) The enriched entries were analyzed based on c2.cp.kegg.v7.1.symbols.gm.

A

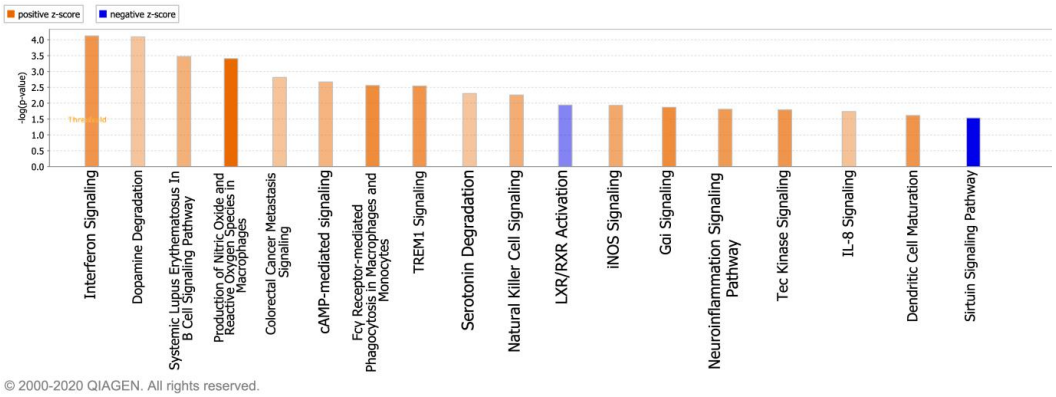




B

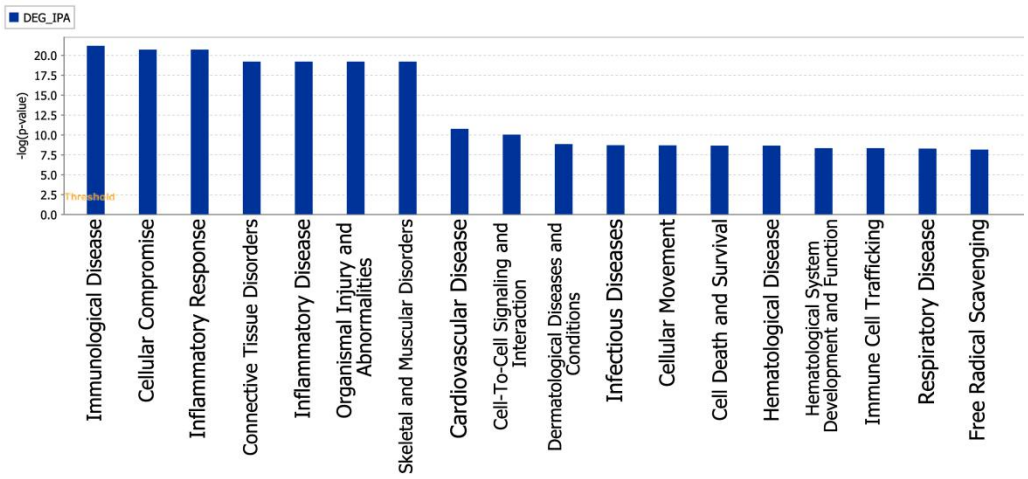

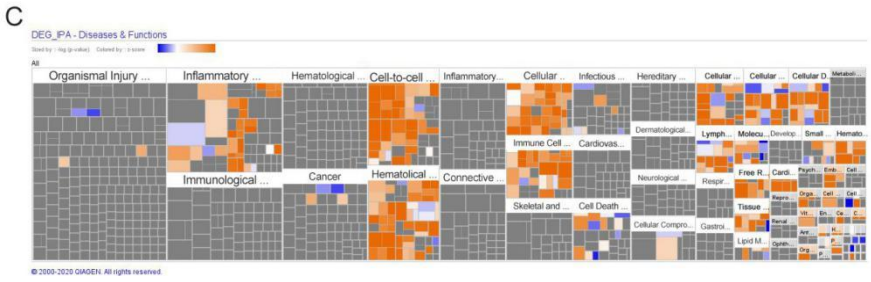


**Figure 3. Canonical pathway and molecule function analysis by IPA.** (A) Canonical pathway analysis by IPA. Orange (*z*-score > 0) and blue (*z*-score < 0). (B) DEGs enriched in the disease and function classification. Enriched disease and function ranked by -log (*p* value). (C) Correlation between DEGs and disease and function. Orange (*z*-score > 0), blue (*z*-score < 0), gray (no *z*-score).

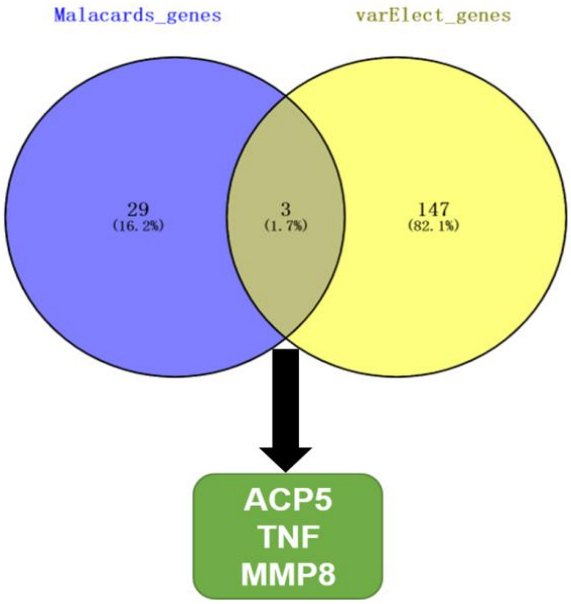


**Figure 4**. Identification of candidate genes of SONFH. Venn diagrams of two gene sets overlapping.

A

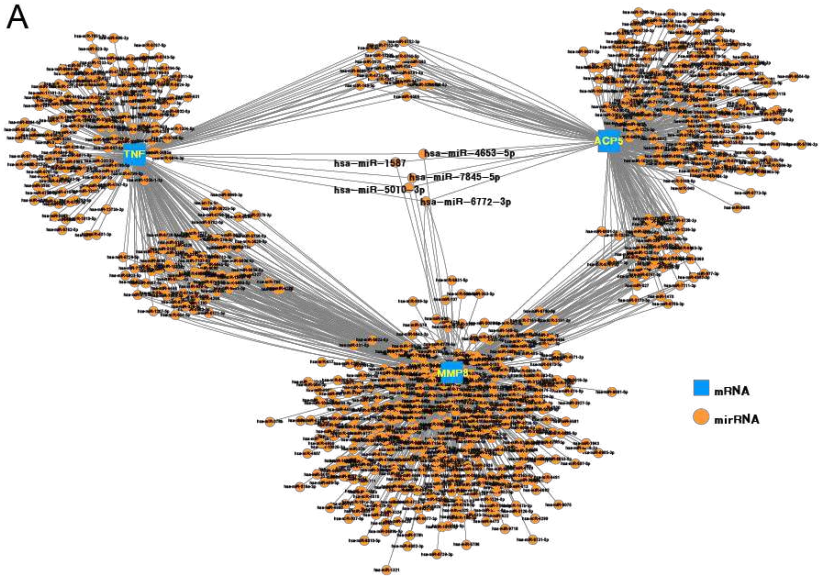
TNF
ACPS
MMP1
hsa-miR-4653-5p
hsa-miR-1587
hsa-miR-7845-5p
hsa-miR-5010-3p
hsa-miR-6772-3p
mRNA
mirRNA

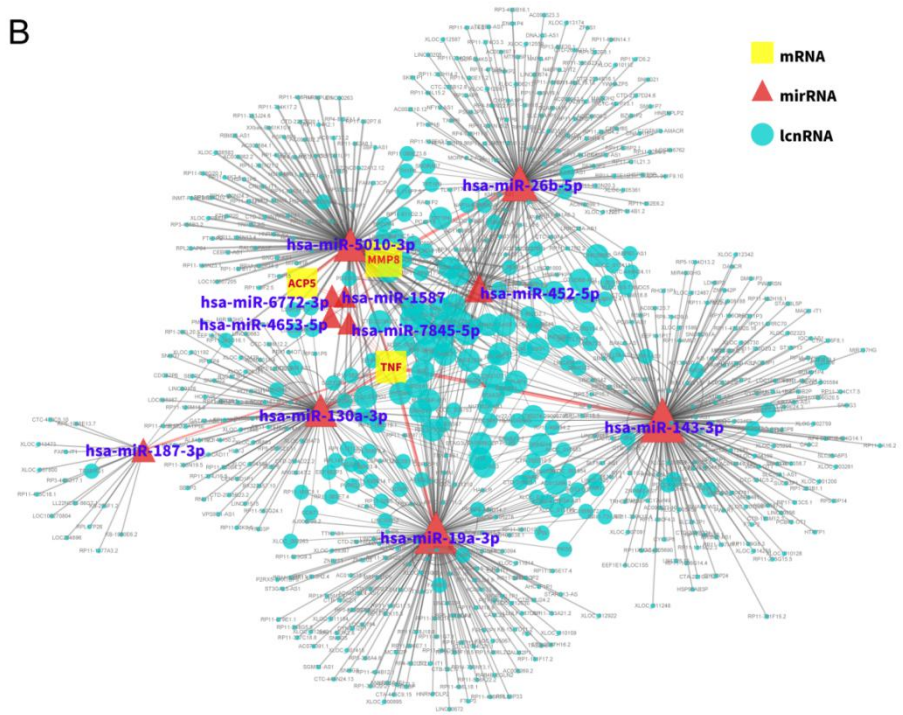


**Figure 5. Construction of ceRNA network of hub genes.** (A) The network between ACP5, TNF, and MMP8 (blue, square) and miRNAs (claybank, round). (B) ceRNA networks among ACP5, TNF, and MMP8 (yellow, square ); miRNAs (red, triangle); and lncRNAs (glaucous, round).